Multiple Roles of the Conserved Key Residue Arginine 209 in Neuronal Nicotinic Receptors†

Francisco Vicente-Agullo,‡,§ Jose C. Rovira,‡,|| Salvador Sala,‡,⊥ Francisco Sala,‡,|| Carmen Rodriguez-Ferrer,# Antonio Campos-Caro,‡,§ Manuel Criado,‡,§ and Juan J. Ballesta*,‡,||

Instituto de Neurociencias, Centro Mixto CSIC-Universidad Miguel Hernández, and Departments of Biochemistry and Molecular Biology, Pharmacology, and Physiology, Universidad Miguel Hernandez, Campus de San Juan, Apartado Correos 18, 03550 San Juan de Alicante, Spain, and Department of Biochemistry and Molecular Biology, Universidad de La Laguna, 38206 La Laguna (Tenerife), Spain

Received January 12, 2001; Revised Manuscript Received April 10, 2001

ABSTRACT: We have examined the role of a highly conserved arginine (R209), which flanks the M1 transmembrane segment of nAChRs, in the biogenesis and function of neuronal nAChRs. Point mutations revealed that, in αBgtx-sensitive neuronal α7 nAChRs, the conserved arginine is required for the transport of assembled receptors to the cell surface. By contrast, R209 does not play any role in the transport of assembled α-Bgtx-insensitive neuronal α3β4 nAChRs to the cell surface. However, a basic residue at this position of α3 and β4 subunits is necessary for either synthesis, folding, or assembly of α3β4 receptors. Moreover, electrophysiological experiments revealed that in α3β4 receptors the conserved arginine of the α3 subunit is involved in either coupling agonist binding to the channel or regulating single channel kinetics.

Several ligand-gated ion channels (LGIC)[1] constitute a gene superfamily that includes the nicotinic acetylcholine receptor (nAChR), the glycine receptor, the 5-HT_3 receptor, and the $GABA_A$ receptor (*1*, *2*). It has been clearly established that the members of this superfamily have a remarkable degree of identity at the level of their primary structures, including several residues conserved in all subunits of all receptors, e.g., cysteine 128, cysteine 142, or arginine 209 (numbering corresponds to the nAChR *Torpedo californica* α1 sequence and will be used hereafter for all subunits). Furthermore, it is also generally accepted that the LGIC share a common overall secondary structure: a long extracellular N-terminal agonist-binding domain followed by four predicted transmembrane segments (M1, M2, M3, and M4) and a short extracellular C-terminal region. Between M3 and M4 there is a cytoplasmic loop that often contains putative regulatory sites of phosphorylation (*1*). In response to specific agonists, LGIC regulate the opening and closing of an ion channel that is an integral part of their structures, inducing a depolarization or hyperpolarization of the membrane, depending on the ionic selectivity of the channel. nAChRs are the best characterized members of the LGIC. Muscle-type nAChRs are pentamers composed of four different subunits with the subunit composition $(\alpha1)_2(\beta1)(\delta)(\gamma \text{ or } \epsilon)$ that bind the snake venom neurotoxin α-Bgtx. Neuronal-type nAChRs that do not bind α-Bgtx are formed from combinations of either α2, α3, α4, or α6 agonist-binding subunits along with β2, β3, β4, and/or α5 structural subunits. Neuronal nAChRs that bind α-Bgtx are formed from homomers of either α7, α8, or α9 agonist-binding subunits. To date no structural subunits for these kinds of neuronal nAChRs have been described (*3*). Recently, a new subunit, α10, has been cloned that forms heterodimers with α9 but is unable to evoke any current when injected alone (*4*).

R209 is an invariant residue flanking the M1 transmembrane segment. It should be close to or line the pore of *Torpedo* nAChRs, as it is labeled by the open channel blocker derivative [^{3}H]quinacrine azide in the open state of the receptor (*5*). Furthermore, mutations of the α1R209 alter the sensitivity of *Torpedo* $\alpha1\beta1\gamma\delta$ nAChRs to quinacrine and determine a large decrease in surface expression of these receptors, suggesting a role of this conserved residue in receptor biogenesis. Interestingly, mutations of the homologous β1R215 only produced a slight reduction in nAChR surface expression (*6*). On the other hand, in theoretical models, R209 has been involved in the molecular events leading to binding of ACh to its receptor (*7*).

† This work was supported by grants from the Ministry of Education (DGICYT, PB95-0690 and PM98-0104) of Spain and Generalitat Valenciana (GV-D-VS-20-158-96). A.C.-C. was the recipient of a CSIC-Bancaja postdoctoral fellowship. F.V.-A. was a recipient of a predoctoral fellowship from the Ministry of Education of Spain.C.R.-F. received a fellowship from Gobierno de Canarias.

* To whom correspondence should be addressed at the Departamento de Farmacologia, Universidad Miguel Hernandez. Telephone: +34-96-591-9486. Fax: +34-96-591- 9492. E-mail: jj.ballesta@umh.es.

‡ Instituto de Neurociencias, Universidad Miguel Hernandez.

§ Department of Biochemistry and Molecular Biology, Universidad Miguel Hernandez.

|| Department of Pharmacology, Universidad Miguel Hernandez.

⊥ Department of Physiology, Universidad Miguel Hernandez.

Department of Biochemistry and Molecular Biology, Universidad de La Laguna.

[1] Abbreviations: ACh, acetylcholine; Bgtx, bungarotoxin; EB, epibatidine; LGIC, ligand-gated ion channel; nAChR, nicotinic acetylcholine receptor; NFR, frog Ringer's solution; PCR, polymerase chain reaction; WT, wild type.

10.1021/bi010087g CCC: $20.00
Published on Web 06/20/2001

To determine the role of this amino acid in the biogenesis and function of neuronal nAChRs, we have performed mutations of this residue in different types of subunits: α-Bgtx-sensitive α7 subunits that form homomers and α-Bgtx-insensitive α3 and β4 subunits that form heterodimers. Results indicated that the effect of mutations is dependent on which type of subunit is mutated. Thus, mutated α7 subunits were unable to reach the oocyte surface. Nonetheless, α7R209K receptors assembled into intracellular pentamers that were similar in binding properties to native receptors. In the case of α3β4 heteromeric nAChRs, most mutations of either α3 or β4 subunits decreased the amount of assembled receptors. However, correctly assembled receptors were transported to the plasma membrane. Only α3R209Kβ4 receptors evoked ionic currents in response to agonist application, although their functional characteristics were different from those of native receptors. Results presented here show that although R209 is conserved in all subunits of LGICs, its role depends on both the type of nAChRs and subunit considered.

EXPERIMENTAL PROCEDURES

Site-Directed Mutagenesis. Point mutations were made by performing two successive PCR amplifications as previously described (*8*, *9*) and were confirmed by sequencing the cDNA clones.

Oocyte Expression. cDNAs of the WT bovine α7, α3, β4 (*9*, *10*) and the corresponding mutated subunits were inserted into the pSP64T vector (*11*). Capped mRNA was synthesized in vitro using SP6 RNA polymerase. Defoliculated *Xenopus laevi* oocytes were injected with 5 ng of total cRNA in 50 nL of sterile water. α3 and β4 were co-injected in an equimolar ratio. All experiments were performed within 3−6 days after cRNA injection.

[^{3}H]EB Binding Assays. The microsomal fraction from *Xenopus* oocytes was obtained as described (*12*) with minor modifications. [^{3}H]EB equilibrium binding to the oocytes microsomal fraction was done as described in Houghtling et al. (*13*). Experimental data were analyzed with LIGAND, a nonlinear least squares computer program (*14*). Surface expression of α3β4 nAChRs was measured as described in Rovira et al. (*15*) by incubating oocytes with 2 nM [^{3}H]EB in the absence (total binding) or presence of 0.5 mM D-tubocurarine (internal binding, since this antagonist cannot permeate the oocyte membrane, as happens with epibatidine). After the incubation, unbound [^{3}H]EB was removed, and oocytes were washed and solubilized. [^{3}H]EB bound to α3β4 nAChRs was measured by precipitating solubilized receptors with mAb 35. The oocyte surface [^{3}H]EB was calculated by subtracting the specific counts per minute obtained for the total and internal binding. Nonspecific binding was determined by using noninoculated oocytes.

[^{125}I]-α-Bgtx Binding Assays. Specific surface expression of [^{125}I]-α-Bgtx binding sites was tested with 5 nM [^{125}I]-α-Bgtx as described (*9*). Briefly, oocytes were incubated with 5 nM [^{125}I]-α-Bgtx. At the end of the incubation, unbound [^{125}I]-α-Bgtx was removed, oocytes were washed, and bound radioactivity was counted. Nonspecific binding was determined using noninoculated oocytes. To measure total [^{125}I]-α-Bgtx binding sites, oocytes were solubilized as described in Anand et al. (*16*), and the oocyte extract was incubated with 5 nM [^{125}I]-α-Bgtx for 2 h. Then the extract was immunoprecipitated with mAb 319, a monoclonal antibody specific for the α7 subunit (*17*).

Sucrose Gradients. For sucrose gradient analysis of AChRs, oocytes expressing subunits were labeled with either [^{125}I]-α-Bgtx or [^{3}H]EB and solubilized. The cleared lysate was layered onto 11 mL sucrose gradients (5−20%) as previously described (*18*). After sedimentation of nAChRs (40 500 rpm, Beckman SW41Ti rotor) at 4 °C for 17 h, 250 μL aliquots were collected and immunoprecipitated with mAb 319 (α7) or mAb 35 (α3β4), and their radioactivity was measured. Control gradients with purified *Torpedo* nAChR were run in parallel.

Electrophysiological Recordings. Electrophysiological recordings were done as previously described (*9*). When ACh was used as agonist, the buffer was supplemented with 0.5 μM atropine.

RESULTS

Expression and Assembly of α7 Subunit Mutants. cRNAs corresponding to either α7R209K or α7R209L mutants were injected into *Xenopus* oocytes, and the specific surface expression of [^{125}I]-α-Bgtx binding sites was measured. In both cases, no receptors were expressed in the oocyte surface (Figure 1A). In the case of the α7R209L mutant no internal binding was evident as well, implying that either the synthesis, folding, or assembly of mutant receptors was impaired. On the contrary, α7R209K receptors displayed internal binding of [^{125}I]-α-Bgtx with a B_{max} that was about 50% of the control (Figure 1B). The K_d of α-Bgtx binding was similar for control and mutated receptors (Figure 1B). Moreover, the size of expressed receptors is consistent with pentameric oligomers, as sucrose gradients of both control and R209K mutated receptors revealed mainly complexes similar to *Torpedo* AChR monomers (Figure 2).

Because no [^{125}I]-α-Bgtx binding sites were detected in the surface of oocytes injected with α7R209K, we could not examine the functional properties of this mutant. However, ligand-binding properties of α7R209K and WT receptors did not reveal any significant difference, as both receptors displayed similar affinities for [^{125}I]-α-Bgtx (Figure 1B) and nicotine (data not shown).

The experiments described above suggest, first, that a positively charged residue at position 209 is needed for proper synthesis and/or assembly of α7 homomeric receptors. In addition, once α7 homomeric receptors are assembled, the specific presence of an arginine residue at position 209 is necessary for them to reach the plasma membrane. This assertion was confirmed when the cRNAs corresponding to α7R209K and WT α7 subunits were co-injected at a 1:1 ratio (Figure 1A). In this case only a small but significant proportion of surface expression of specific [^{125}I]-α-Bgtx binding sites was observed (16.3 ± 1.8% of control). This suggests that mutant subunits were able to recognize and assemble with WT ones, but the former would inhibit further transport of assembled receptors. According to a simple probability estimation, and taking into account the amount of receptors which reach the membrane, these would have a stoichiometry of either five wild-type subunits or four of them assembled with one α7R209K mutant subunit. These receptors produced ionic currents when oocytes were chal-

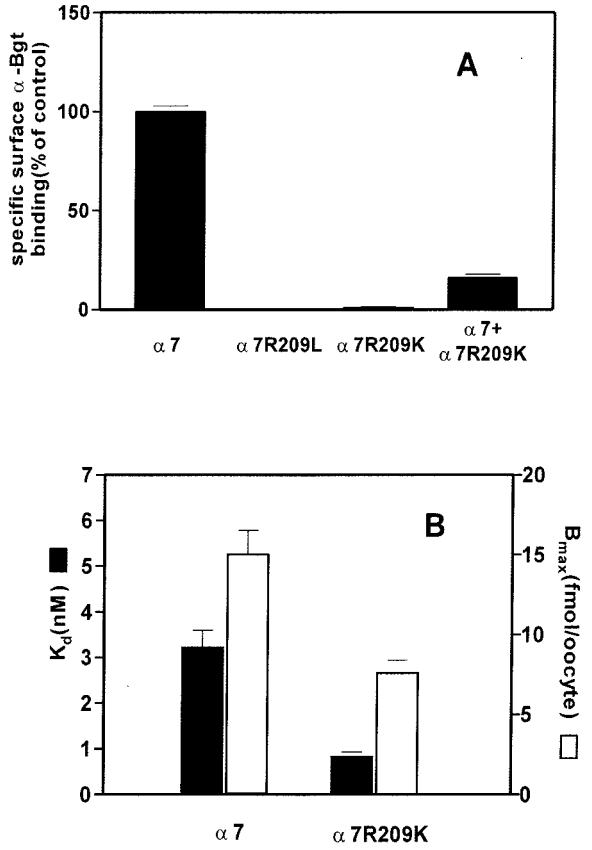

FIGURE 1: [^{125}I]-α-Bgtx surface expression on intact oocytes and parameters of equilibrium binding to the oocytes microsomal fraction. (A) [^{125}I]-α-Bgtx specific surface binding was measured in oocytes injected with the corresponding cRNAs. In the case of oocytes co-injected with α7 and α7R209K, cRNAs were injected in a 1:1 ratio. Data were normalized to those obtained with the α7 subunit, and means ± SEM of at least three experiments from different donors (20 oocytes/experiment) are shown. (B) K_d (solid columns) and B_{max} (open columns) of [^{125}I]-α-Bgtx binding to solubilized oocytes expressing either α7 or α7R209K. Experimental data from two saturation experiments from different donors were adjusted by the LIGAND program.

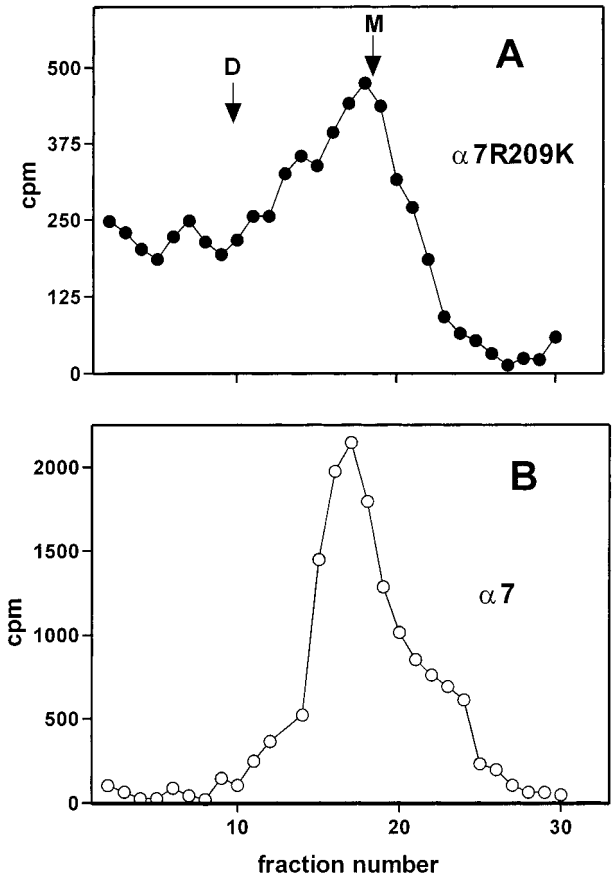

FIGURE 2: Sedimentation profile on a 5−20% sucrose gradient of [^{125}I]-α-Bgtx-labeled α7R209K (A) and α7 (B) subunits expressed in oocytes injected with the corresponding cRNAs. The arrows indicate the position of *Torpedo* nAChR monomers (M) and dimers (D) run in a parallel experiment.

lenged with ACh. When currents were normalized to [^{125}I]-α-Bgtx surface expression, they were similar to the ones obtained with normal α7 receptors, suggesting that they have their functional properties intact.

Expression and Assembly of α3 and β4 Subunit Mutants. cRNAs corresponding to equimolar combinations of α3 and β4 subunits mutated or not at the mentioned arginine were injected into *Xenopus* oocytes, and the specific expression of [^{3}H]EB binding sites was measured. In oocytes expressing α3R209Kβ4 nAChRs, the total and external expression of [^{3}H]EB binding sites was similar to that of WT receptors (Figure 3). Therefore, and contrary to what happened with α7R209K homomeric receptors, neither assembly nor transport was impaired. However, substitution of α3R209 to negatively charged or neutral residues led to a reduction in the number of assembled receptors. Thus, assembly of α3R209Eβ4 receptors was reduced by 80% (Figure 3A), with a slight decrease in the transport of receptors to the oocyte plasma membrane (Figure 3B). The decrease in the number of assembled receptors was even larger when α3R209 was mutated to aliphatic amino acids. For instance, no [^{3}H]EB binding sites were detected in oocytes co-injected with α3R209L and β4, whereas the assembly of α3R209Aβ4 receptors was only 10% of the control (Figure 3A). In this case, the transport of assembled receptors to the oocyte plasma membrane was reduced by 30% with respect to WT (Figure 3B). It can be concluded that, in the α3 subunit of heteromeric α3β4 nAChRs, the properties of the residue located at position 209 determine the efficiency of receptor biogenesis. Once receptors are assembled, the transport to the plasma membrane is largely independent of the nature of the amino acid at this position. Sucrose gradient experiments showed that α3R209Kβ4 nAChRs were pentameric (Figure 4A) and have sedimenting profiles similar to those of wild-type receptors (Figure 4C).

Next, we asked whether the analogous position at the β4 subunit would also be important in this process. In the case of α3β4R209K, assembly decreased by 40% (Figure 3A), while the efficiency of transport to the cell surface was unaltered (Figure 3B). Surprisingly, some specific [^{3}H]EB binding sites were detected when β4R209L was coexpressed with α3, about 30% of the native receptors (Figure 3A), with no change in the extent of transport of assembled receptors to the plasma membrane (Figure 3B). These mutant receptors appeared to be pentamers as they had the same sedimenting profiles as the WT (panels B and C of Figure 4, respectively).

At this point, it was tempting to explain the different cell surface transport properties of homomeric α7R209K nAChRs and the corresponding heteromeric mutant α3β4 nAChRs by the fact that the former has five mutated subunits whereas

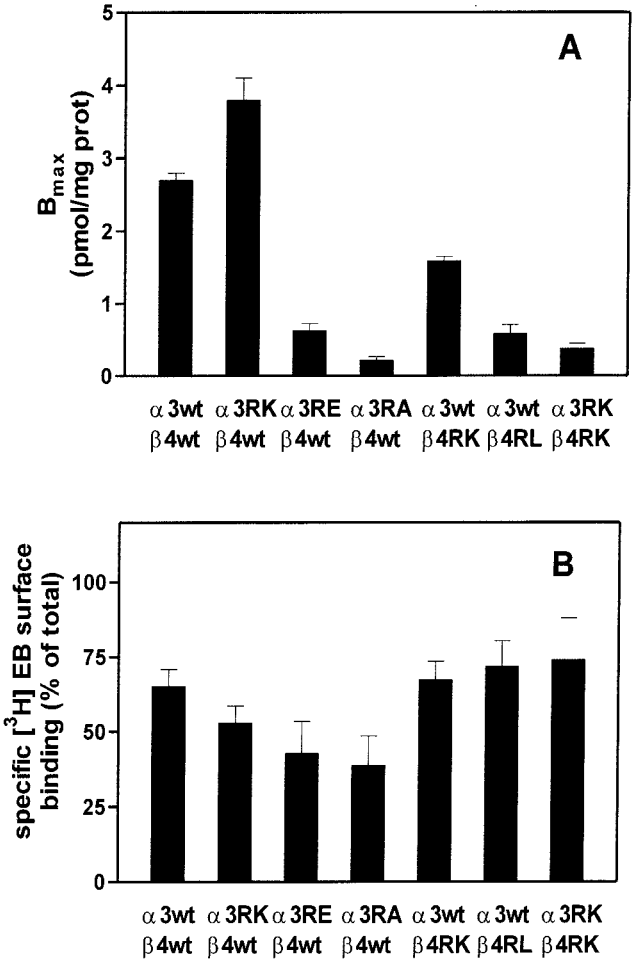

FIGURE 3: [^{3}H]EB binding to oocytes expressing different combinations of WT and mutated α3β4 nAChRs. (A) B_{max} of specific [^{3}H]EB binding to the oocyte microsomal fraction was obtained from saturation experiments of oocytes injected with the corresponding cRNAs. Data from at least two duplicate experiments were adjusted by the program LIGAND. (B) [^{3}H]EB specific oocyte surface binding was normalized to the total specific binding (B_{max}) and is represented as means ± SEM of at least three experiments from different donors.

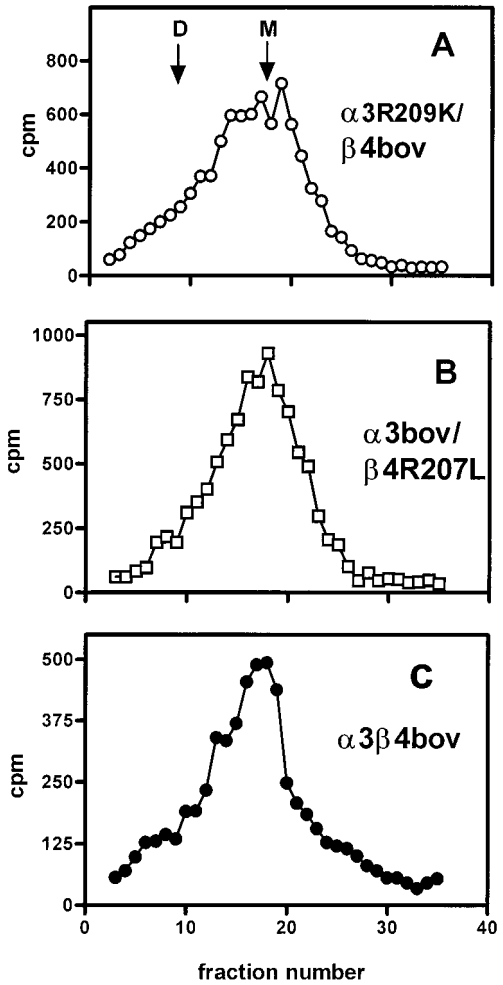

FIGURE 4: Sedimentation profile on a 5−20% sucrose gradient of [^{3}H]EB-labeled α3R209Kβ4 (A), α3R209Lβ4 (B), and α3β4 (C) nAChRs expressed in oocytes injected with the corresponding cRNAs. The arrows indicate the position of *Torpedo* nAChR monomers (M) and dimers (D) run in a parallel experiment.

the latter has only two or three. An alternative hypothesis would be that the role of R209 in the transport of nAChR to the cell surface depends on the type of receptor: R209 would play a pivotal role in the transport of α7 homomeric receptors but not in that of α3β4 heteromeric receptors. To address this issue, we co-injected α3R209K and β4R209K and measured total and cell surface expression of [^{3}H]EB binding sites. Results showed that the number of assembled α3R209Kβ4R209K nAChRs was drastically decreased, being only 10% of the control (Figure 3A). However, the transport to the oocyte surface of the few receptors which were expressed was unaltered (Figure 3B). These results suggest that the effect of changing the arginine residue at position 209 of neuronal nAChRs on the biogenesis and transport to the cell surface depends on the type of receptor and is unrelated to the number of mutated subunits. Thus, in homomeric α7 receptors it determines the extent of transport of assembled receptors to the cell surface, whereas in heteromeric α3β4 nAChRs it controls their biogenesis.

Function and Pharmacology of α3 and β4 Mutated Receptors. After co-injection of the cRNAs corresponding to β4 with either α3R209K, α3R209E, α3R209L, or α3R209A, only α3R209Kβ4 receptors elicited detectable macroscopic currents upon pulse application of different nicotinic agonists (Figure 5A). Agonist-evoked ionic currents in oocytes expressing α3R209Kβ4 receptors showed, when compared with WT receptors, (1) a decrease in the peak current evoked by either ACh, nicotine, or EB and (2) an increase in the rate of macroscopic desensitization upon stimulation with low, as well as high, agonist concentrations (WT receptors displayed a small desensitization component only at high agonist concentrations) (Figure 5A). Having taken into account the fact that the expression of α3R209Kβ4 nAChRs was similar to that of native receptors, the drastic reduction of functional responses in α3R209Kβ4 nAChRs could be explained by at least one of the following changes: (a) an increase in the rate of desensitization, (b) impaired binding of nicotinic agonists, (c) impaired gating, and (d) reduced single channel conductance. These possibilities are addressed in turn. The fast macroscopic desensitization component displayed by α3R209Kβ4 nAChRs accounts for an underestimation of the peak currents. In any case, the desensitization of mutated receptors cannot explain the observed reduction in the peak current. To check for a possible effect of the mutation on the apparent affinity of

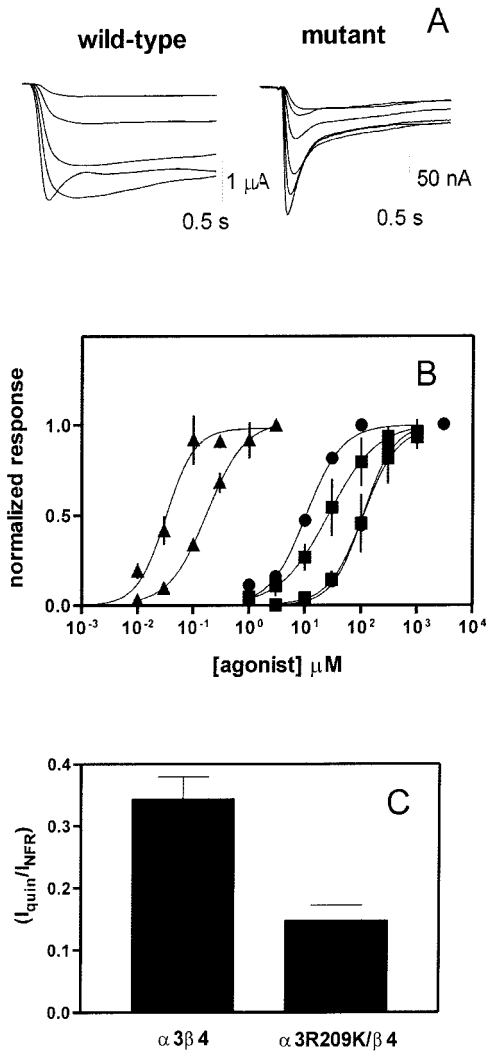

FIGURE 5: Pharmacological profile of oocytes expressing α3*β*4 and α3R209K*β*4 nAChRs. (A) Macroscopic currents obtained upon challenging oocytes with 10 *μ*M−3 mM (WT) or 1 *μ*M−0.3 mM nicotine (α3R209K/*β*4). (B) Dose−response curves of macroscopic currents performed in oocytes expressing WT (open symbols) and α3R209K/*β*4 nAChRs (filled symbols) stimulated with EB (▲), nicotine (●), and ACh (■). Currents were normalized to the maximal response and represent means ± SEM of 4−12 experiments from at least two donors. (C) Blockade by 30 nM quinacrine of whole membrane currents evoked by 100 *μ*M nicotine in oocytes expressing α3/*β*4 and α3R209K/*β*4 nAChRs. Currents challenged in the presence of quinacrine were normalized to currents obtained upon stimulation by nicotine alone. Results represent means ± SEM of five oocytes from two donors.

the receptor for nicotinic agonists, we carried out macroscopic dose−response curves (Figure 5B). Results showed a decrease in the EC_{50}'s of mutated receptors for ACh, nicotine, and EB. Furthermore, apparent K_d's of [^{3}H]EB and K_i's of ACh, nicotine, and D-tubocurarine in displacing [^{3}H]-EB binding were similar in native and α3R209K*β*4 receptors (data not shown). As the expression of native and mutated receptors at the oocyte surface was similar, the alteration in macroscopic currents produced by the mutation could be due to an impairment of the coupling between agonist binding and channel activation or modification of single channel properties. It was not possible to rule out any of these possibilities given that no single channel currents of mutated receptors could be detected, although in α3*β*4 receptors measurements of single channel currents are feasible (*15*).

As previously mentioned, neither α3R209E, α3R209A, nor α3R209L co-injected with *β*4 evoked any detectable current when nicotine was applied at concentrations up to 3 mM nicotine. Furthermore, nicotine-challenged macroscopic currents were also absent in oocytes injected with the combinations α3*β*4R209K, α3*β*4R209L, and α3R209K*β*4R209K. As K_d's of [^{3}H]EB in these mutant nAChRs were similar to the K_d's in native receptors (data not shown), the lack of macroscopic currents is most likely due to either the reduced surface expression of these mutated nAChRs (except α3*β*4R209K nAChRs), a decrease in the elementary conductance or the open probability of the receptors, or a combination of both.

The differential sensibility to the open channel blocker quinacrine has been previously used to conclude that arginine 209 lines the channel of *Torpedo* nAChRs (*5*, *6*). The same situation could be true for neuronal nAChs, and therefore, we measured the ionic responses of α3*β*4 and α3R209K*β*4 nAChRs to ACh applied alone or in the presence of quinacrine. As shown in Figure 5C, α3R209K*β*4 receptors were more sensitive to the inhibition by quinacrine than native receptors. These results are consistent with the localization of R209 in the ion pore of neuronal nAChRs.

DISCUSSION

In the present study we have characterized the role of the conserved amino acid arginine 209 on the biogenesis and transport of neuronal α-Bgtx-sensitive homomeric α7 receptors and α-Bgtx-insensitive heteromeric α3*β*4 receptors. Point mutation data showed that, in homomeric α7 receptors, R209 is essential for the transport of assembled receptors to the plasma membrane. By contrast, in heteromeric α3*β*4 nAChRs, the conserved arginine does not display any role in the transport of assembled receptors to the plasma membrane. Instead, it affects the biogenesis of receptors. In addition, α3R209 plays a functional role in agonist-induced macroscopic currents.

We assume that specific intracellular [^{125}I]-α-Bgtx binding sites detected in oocytes expressing α7R209K represent fully assembled pentameric receptors because (a) the apparent affinities of nicotine and [^{125}I]-Bgtx in α7R209K nAChRs are similar to WT ones and (b) sucrose gradient centrifugation experiments demonstrated that both α7 and α7R209K nAChRs sedimented at ∼10 S, although the sedimentation profile of α7R209K evidenced some larger aggregates. These data are in agreement with a previous report that demonstrated that only fully assembled chick α7 pentamers are able to bind [^{125}I]-Bgtx with high affinity (*16*). Although the total number of assembled α7R209K receptors was decreased by 50%, it is much more striking that surface expression of these mutated receptors was entirely abolished. Thus, it is likely that the mutant α7R209K has lost a membrane export signal or, alternatively, acquired a retention signal that prevents assembled receptors from reaching the cell membrane. Previously, it has been demonstrated that a double arginine motif located near the N-terminus (*20*, *21*) and a cytoplasmic loop RKR motif (*22*) direct the retention/retrieval of proteins to the ER. In the case of the RKR motif of ATP-sensitive K^+ channels, it has been shown that both RKR and RRR sequences induce the retention of subunits in the ER (*22*).

α7 nAChRs display two clear differences with respect to the cytoplasmic loop RKR motif of the mentioned K^+ channel: (a) the RRR sequence of WT α7 subunits does not retain fully assembled receptors in the ER, and (b) RRR and, presumably, RKR residues in the case of mutated α7 receptors are located in the extracellular side of the protein, far away from the N-terminus and just before the beginning of the M1 transmembrane domain, according to the current topological model of nAChRs (*1*). Thus, although the putative retention/retrieval sequence we have identified is composed of basic residues as the previous reported sequences (*20*, *21*, *22*), it is clearly different in both its location and specific amino acid requirements. An alternative hypothesis is that α7R209K subunits have not acquired a retention signal, but a conformational change has occurred in other regions of the protein that inhibits transport of assembled nAChRs to the cell surface by hindering molecular interactions with the transport machinery. This would be the case if the mutated residue, which lines the pore of the receptor (*5*, *6*), was inaccessible to retention proteins after assembly. Regarding α3β4 heteromeric receptors, it is noteworthy that the transport to the cell surface of assembled R209 mutants in both subunits was not affected, suggesting that the mentioned residue is not involved in the transport process. However, expression of assembled α3β4 nAChRs is largely dependent on the properties of the residue at position 209. Thus, changes of R209 by negatively charged or neutral amino acids in any of the subunits led to a reduction in the number of expressed receptors, as compared with WT, α3R209Kβ4, and α3β4R209K nAChRs. In the case of R209K mutants, results suggest that the expression of nAChRs is determined by the number of lysine residues present at position 209. Thus, the expression of α3R209Kβ4 nAChRs (two lysine residues) was fairly similar to that of WT receptors; meanwhile, that of α3β4R209K nAChRs (three lysine residues) was slightly reduced (60% of control) and that of α3R209Kβ4R209K nAChRs (five lysine residues) was largely decreased (15% of control).

Taking together results from α7 and α3β4 receptors, it is evident that arginine 209 has a nonequivalent role in the assembly and transport of different types of neuronal nAChRs. It can also be suggested that the ability of α7R209K to prevent fully assembled receptors to reach the cell surface is influenced by some other properties of the protein.

Concerning functional expression of mutated α3β4 heteromeric receptors, only α3R209Kβ4, but not α3β4R209K, nAChRs displayed detectable currents when challenged with nicotinic agonists, illustrating that R209 plays nonequivalent functional roles in α3 and β4 subunits. The functional role of R209 is also dissimilar between different ACh-binding subunits and also between different structural subunits. Thus, α1R209Kβ1γδ receptors show, when compared with WT, an increase in the current amplitude in response to ACh (*6*). On the contrary, our results demonstrate that when α3R209Kβ4 nAChRs are challenged with nicotinic agonists, the amplitude of the current largely decreases and the rate of macroscopic desensitization increases (Figure 5A). The role of R209 is also nonequivalent between different structural subunits, as α1β1R215Kγδ nAChRs do not display any functional difference with respect to WT ones (*6*), but α3β4R209K nAChRs were functionally inactive, despite the fact that its surface expression was reduced only by 35%, as compared to WT receptors. However, as the stoichiometry of neuronal nAChRs is $(\alpha3)_2(\beta4)_3$ (*16*), an alternative explanation is that the number of arginine residues at position 209 is critical for the function of the receptor. If this is true, receptors with two mutated residues at position 209 (α3 R209Kβ4) would be functional, whereas receptors with three mutated residues at that position (α3β4 R209K) would be nonfunctional.

As mentioned above, agonist-evoked ionic currents in oocytes expressing α3R209Kβ4 receptors showed a large reduction of the macroscopic current and an increase in the rate of desensitization, when compared with WT receptors. As discussed before, the altered function of these mutated receptors must be due either to an impairment of the coupling between agonist binding and gating or to modification of single channel properties. This is not surprising since the arginine residue is located just before the M1 transmembrane segment, which lines the pore, as has been previously demonstrated for muscle type nAChRs (*5*) and has also been evidenced in the present paper by the increased sensitivity of α3R209Kβ4 receptors to inhibition by the open channel blocker quinacrine. In any case it is obvious that R209 plays a very important role in the function of neuronal α3β4 nicotinic receptors.

ACKNOWLEDGMENT

We thank Mrs. Eva Martinez for technical assistance and Dr. Jon Lindstrom for the generous gift of mAb 35 and mAb 319. This paper is in memory of the late Dr. Alfredo Orts.

REFERENCES

1. Cockcroft, V. B., Osguthorpe, D. J., Barnard, E. A., Friday, A. E., and Lundt, G. G. (1992) *Mol. Neurobiol. 4*, 129−169.
2. Jackson, M. B., and Yakel, J. L. (1995) *Annu. Rev. Physiol. 57*, 447−468.
3. Chen, D., and Patrick, J. W. (1997) *J. Biol. Chem. 272*, 24024−24029.
4. Elgoyhen, A. B., Vetter, D. E., Katz, E., Rothlin, C. V., Heinemann, S. F., and Boulter, J. (2001) *Proc. Natl. Acad. Sci. U.S.A. 98*, 3501−3506.
5. Karlin, A. (1991) *Harvey Lect. Ser. 85*, 71−107.
6. Tamamizu, S., Todd, A. P., and McNamee, M. G. (1995) *Cell. Mol. Neurobiol. 15*, 427−438.
7. Aprison, M. H., Galvez-Ruano, E., and Lipkowitz, K. B. (1996) *J. Neurosci. Res. 46*, 226−230.
8. Hertzlize, S., and Koenen, M. (1990) *Gene 91*, 143−147.
9. García-Guzman, M., Sala, F., Sala, S., Campos-Caro, A., and Criado, M. (1994) *Biochemistry 33*, 15198−15203.
10. Campos-Caro, A., Smillie, F. I., Dominguez del Toro, E., Rovira, J. C., Vicente-Agullo, F., Chapuli, J., Juiz, J. M., Sala, S., Sala, F., Ballesta, J. J., and Criado, M. (1997) *J. Neurochem. 68*, 488−497.
11. Krieg, P. A., and Melton, D. A. (1984) *Nucleic Acids Res. 12*, 7057−7070.
12. Buller, A. L., and White, M. M. (1992) *Methods Enzymol. 207*, 368−375.
13. Houghtling, R. A., Davila-García, M. I., and Kellar, K. J. (1995) *Mol. Pharmacol. 48*, 280−287.
14. Munson, P. J., and Rodbard, D. (1980) *Anal. Biochem. 107*, 220−239.
15. Rovira, J. C., Ballesta, J. J., Vicente-Agullo, F., Campos-Caro, A., Criado, M., Sala, F., and Sala, S. (1998) *FEBS Lett. 433*, 89−92.
16. Anand, R., Conroy, W. G., Schoepfer, R., Whiting, P., and Lindstrom, J. (1991) *J. Biol. Chem. 266*, 11192−11198.

17. Schoepfer, R., Conroy, W. C., Whiting, P., Gore, M., and Lindstrom, J. (1990) *Neuron 5*, 35−48.
18. Criado, M., and Barrantes, F. J. (1984) *Biochim. Biophys. Acta 798*, 374−381.
19. Anand, R., Peng, X., and Lindstrom, J. (1993) *FEBS Lett. 327*, 241−246.
20. Schutze, M. P., Peterson, P. A., and Jackson, M. R. (1994) *EMBO J. 13*, 1696−1705.
21. Hui, N., Nakamura, N., Sönnichsen, B., Shima, D. T., Nilsson, T., and Warren, G. (1997) *Mol. Biol. Cell 8*, 1777−1787.
22. Zerangue, N., Schwappach, B., Jan Y. N., and Jan, L. Y. (1999) *Neuron 22*, 537−548.
23. Teasdale, R. D., and Jackson, M. R. (1996) *Annu. Rev. Cell Dev. Biol. 12*, 27−54.

BI010087G